Wind-Tunnel Studies of Wing Wake Turbulence

N. A. CHIGIER* AND V. R. CORSIGLIA†
NASA Ames Research Center, Moffett Field, Calif.

Velocity measurements have been made in the wake of wings in the Ames 7- By 10-Foot Wind Tunnel. Distributions of velocity components were measured with a three-wire anemometer up to 12 chord lengths downstream of CV-990 aircraft model and a rectangular wing. Results show that increasing the drag increases the vortex core radius, reduces the maximum tangential velocities and increases the magnitude of axial velocity defects. For the rectangular wing, axial velocity changes from a defect (wake flow) for $\alpha < 9°$ to an excess (jet flow) for $\alpha > 9°$. Wind-tunnel measurements of the near-flowfield are compared with flight measurements of the far-flowfield.

Nomenclature

a = core radius—radius where u_θ is a maximum
b = wing span
c = wing chord
C_L = lift coefficient
r = radial coordinate from vortex center
S = wing surface area
TI = turbulence intensity, $(\overline{u'_x{}^2} + \overline{u'_y{}^2} + \overline{u'_z{}^2})^{1/2}/(\bar{u}_x{}^2 + \bar{u}_y{}^2 + \bar{u}_z{}^2)^{1/2}$ (primes indicate instantaneous quantities, bars indicate means)
u_x = axial velocity component
u_θ = tangential velocity component
V_∞ = wind-tunnel mainstream velocity
x = streamwise ordinate, aft from trailing edge
y = spanwise ordinate, inboard from wing tip
y_c = spanwise location of vortex center
z = normal ordinate, above upper wing surface from trailing edge
z_c = normal location of vortex center
α = angle of attack, deg
ω = angular velocity

Subscripts
max = maximum value at a particular axial station
min = minimum value at a particular axial station

Introduction

TRAILING vortices from large aircraft persist for several minutes after generation and present a hazard to smaller aircraft that might intersect their path. Also, tip vortices shed from helicopter rotor blades interact with following blades causing rotor noise and vibration. To reduce the vortex hazard and interaction it is desirable to develop an understanding of vortex structure and dissipation with the ultimate aim of causing a significant reduction in vortex velocities in the wake of aircraft and rotor blades.

The exact nature of trailing vortices has not been clearly established. All analytical and numerical prediction methods require reliable experimental evidence to test the validity of the assumptions and approximations used in making the predictions. A qualitative picture of trailing vortices has been established previously by smoke visualization studies[1] but, with the notable exception of the early work of Fage and Simmons,[2] very few direct measurements of velocity have been made in the wake of wings.

Detailed measurements were made of velocity, turbulence, and surface pressures to determine the flowfields in the near wake region, including the formation and roll-up regions of trailing vortices, and thereby delineate the boundaries and strength of 1) rigid body vortex cores and associated axial flow and 2) the potential flow region. Velocity measurements were made with a three-wire hot wire anemometer in the Ames 7- By 10-Foot Wind Tunnel. Two models have been tested: a rectangular wing having an NACA 0015 airfoil section with a square tip, and a semispan model of the NASA-Ames Convair 990 aircraft with fuselage, open engine nacelles, and flaps. For each model, spanwise and normal distributions of longitudinal, spanwise, and normal velocity components were measured through the vortex centers. Effects of the variation of angle of attack from 4°–16° and the variation of axial distance up to 12 chord lengths downstream of the models were investigated.

The authors have reported previously on the vortex wake effects of a small spoiler on the tip of a rectangular wing and a Convair 990 aircraft.[3] Surface pressure and velocity distributions at one angle of attack up to four chord lengths downstream of the rectangular wing were reported to the 27th Annual National V/STOL Forum of the American Helicopter Society in May 1971 (Ref. 4). A listing of all measured data together with details of test procedure and conditions, and data reduction methods are being published concurrently with this paper in Ref. 5. Kuhn and Nielsen[6] have compared experiments with theoretical predictions based on the measurements made by the authors of this paper.

Apparatus

Tests were conducted in the Army and NASA Ames 7- By 10- Foot Wind Tunnels. The dimensions and geometry of the rectangular planform wing semispan model and the Convair 990 semispan model are listed in Table 1.

Table 1 Model geometry

	Rectangular wing	CV-990 wing
Semispan	121.8 cm (48 in.)	91.5 cm (36 in.)
Reference chord, $c = S/b$	45.7 cm (18 in.)	31.5 cm (12.4 in.)
Aspect ratio	5.33	6.2
Section root	NACA 0015	NACA 001-64
tip	NACA 0015	NACA 0008-64
Incidence root	0°	4°
tip	0°	2°
Trailing edge flap	None	Plain, deflection 27°

Presented as Paper 72–41 at the AIAA 10th Aerospace Sciences Meeting, San Diego, Calif., January 17–19, 1972; submitted February 14, 1972; revision received July 31, 1972. The authors wish to thank M. Kelly, Chief of the Large Scale aerodynamics Branch at Ames for many helpful suggestions and discussions and also J. Frick for valuable assistance in computation.

Index categories: Jets, Wakes, and Viscid Inviscid Flow Interaction; Viscous Nonboundary-Layer Flows.

* National Research Council Senior Associate 1970/71.
† Research Scientist. Member AIAA.

The vortex wake was surveyed with a hot wire probe[4] consisting of three wires placed in a three-axis array operated by three separate constant-temperature anemometers. Measurements were effectively averaged over a region 2 mm in diameter. Traverses were made parallel and normal to the spanwise direction through the vortex centers, using a remotely controlled traversing mechanism, with the probe retained at successive points for a period of time sufficient to take averages. Each wire of the probe was calibrated as a function of wind tunnel speed before and after several traverses. Measured mean voltages were corrected for local measured air temperature variation. Magnitudes of streamwise, spanwise, and normal velocity components were calculated from measured time average dc voltage.

Analysis of the Measurements

The results obtained from the rectangular wing will be discussed first followed by results from the CV-990 model. Characteristic results have been selected from the measured data[5] that show the more significant effects of the vortex structure and the influence of varying angle of attack and axial distance.

Rectangular Wing

The flowfield in the wake is dominated by the swirling motion. The measured distribution of the tangential velocity component (Fig. 1) shows the core to be linear, with $u_\theta = \omega r$, surrounded by a potential region with u_θ inversely proportional to r. The distribution of axial velocity component (Fig. 2) shows that axial velocity gradients are mainly confined to the central core region with velocities below (defect) or above (excess) wind-tunnel mainstream velocity V_∞ according to spatial position and angle of attack. These profiles are typical of those measured throughout the study, so subsequent discussion in this paper will be confined to the characteristic velocities $u_{\theta\ \max}$, $u_{x\ \max}$ or $u_{x\ \min}$ and a, the core radius of each measured traverse.

As the angle of attack increases, the increase in lift force is expected to result in increased vortex strength. Reference 9 states that the circulation at the core radius is a constant fraction of the vortex strength and that the normalized velocity is proportional to the lift coefficient. Figure 3 shows that for over the range of α from 4° to 12°, $u_{\theta\ \max}$ increased linearly with α and there was no significant change in the core radius. An increase in lift leads to an increase in magnitude of the swirl velocity without any significant change in the form of the profile.

It has generally been expected that axial flow in the core would, under flight conditions, be towards the aircraft and therefore, under wind-tunnel conditions axial velocities would

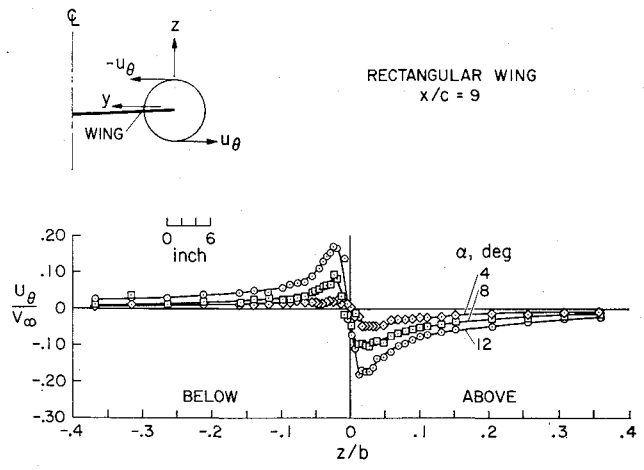

Fig. 1 Tangential velocity distributions. Rectangular wing, normal traverse at $x/c = 9.0$ showing effect of variations of α.

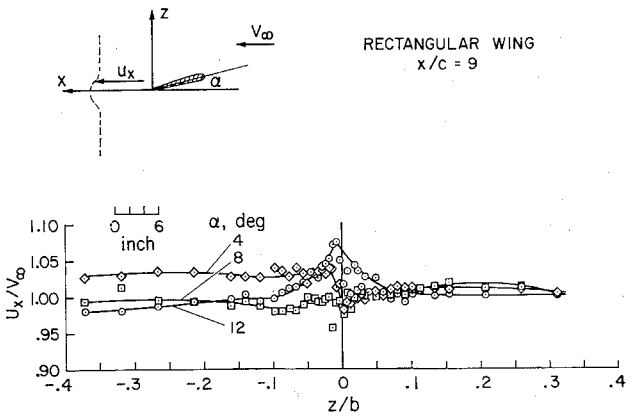

Fig. 2 Axial velocity distributions. Rectangular wing, normal traverse at $x/c = 9.0$ showing effect of variation of α.

be less than V_∞. The measurement of the peak values of axial velocity (Fig. 3) shows that for $\alpha = 8°$ and less the axial velocity was less than V_∞, and at $\alpha = 12°$ the axial velocity exceeded V_∞. It is not clear why such a variation should take place but Batchelor[7] has predicted the possibility of axial flows in directions both towards and away from the wing. Axial velocity defects are associated with drag whereas axial velocity excesses are associated with acceleration over the wing surface as well as axial pressure gradients. It should be noted that vortex breakdown is generally accompanied by axial flow reversal and the results on Fig. 2 showing that axial flow direction can be changed by varying α may indicate a practical means of inducing vortex breakdown.

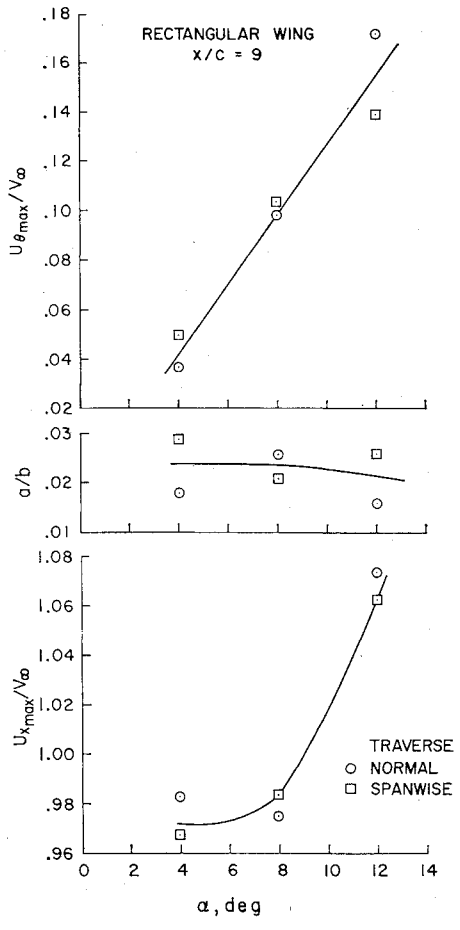

Fig. 3 Rectangular wing, effect of variation of α on $u_{\theta\ \max}$, a, and $u_{x\ \max}$, at $x/c = 9.0$.

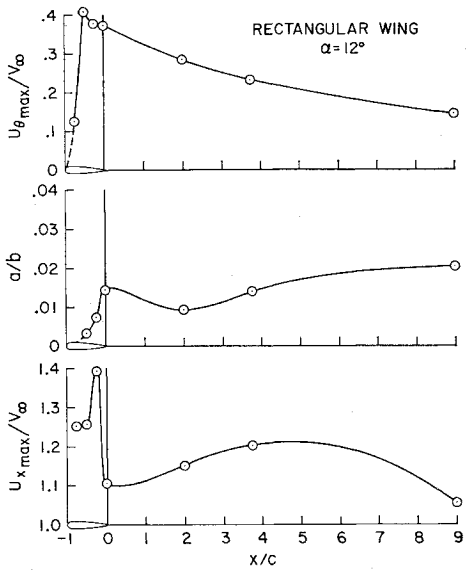

Fig. 4 Rectangular wing, effect of variation of axial distance on a, $u_{\theta\ max}$, and $u_{x\ max}$, at $\alpha = 12°$.

Very little information has hitherto been available about downstream variation of vortex strength and size. Reports of persistence of trailing vortices up to 15 miles behind the C5A aircraft as well as visualization of smoke and vapor trails show that changes and decay in the downstream direction can be at a very slow rate. For measurements in wind tunnels, the length of the test section limits the distances downstream of the wing that can be investigated. Figure 4 shows the effect of variation of axial distance up to a distance of nine chord lengths behind the trailing edge. The $u_{\theta\ max}$ reaches a maximum value over the wing surface and subsequently decays to a value of $u_{\theta\ max}/V_\infty = 0.14$. Core radius is of the order of 2% of the span. After initial changes associated with the roll-up process, core radius increases corresponding to $u_{\theta\ max}$ decay. The axial velocity variations shown in Fig. 4 can be explained as being initially influenced by the accelerating flow over the wing surface, followed by an interaction with the turbulent wake at the trailing edge. The "reflected image" of core radius variation compared to axial velocity variation with axial distance could be interpreted as being due to a dynamic confinement of the axial flow with accelerations and decelerations corresponding to decreases and increases in core diameter.

The location of the local center, as determined by the position of zero tangential velocity, was determined from the span-

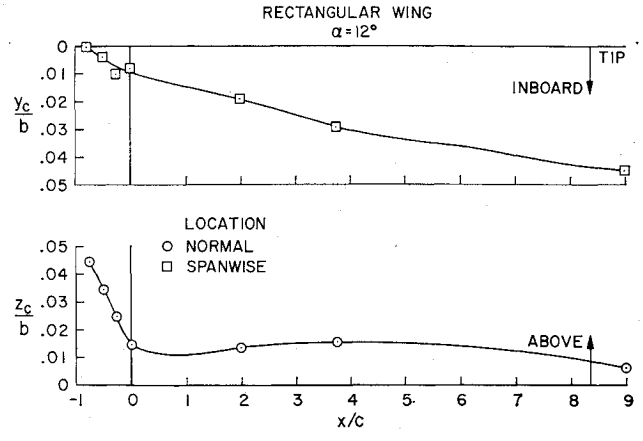

Fig. 5 Rectangular wing, spanwise and normal location of vortex centerline as a function of axial distance at $\alpha = 12°$.

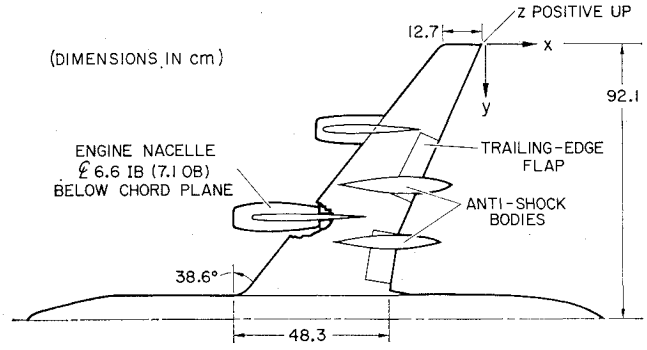

Fig. 6 Model of CV-990 aircraft (semispan) showing location of engine nacelles, antishock bodies and flaps.

wise and normal traverses at each axial station. These locations are plotted as a function of axial distance x/c in Fig. 5. The vortex center moved inboard from the tip as a consequence of the nonuniform spanwise load distribution and reached a value of $y_c/b = 0.05$ at $x/c = 9$.

Downwash is determined by the interaction of a vortex pair. Since the single vortex of the present study was located close to the wind tunnel centerline; the location of the vortex center was influenced by the image vortices from all four walls of the 7- By 10-Foot Wind Tunnel. The normal location of the vortex center (Fig. 5) shows that even up to $x/c = 9.0$ the vortex center was located above the trailing edge.

CV-990 Aircraft Model

The semispan model of the NASA-Ames Convair 990 jet transport aircraft is shown in Fig. 6. The model has a swept, tapered, twisted wing with fuselage, open engine-nacelles, antishock bodies, and flaps. Over-all dimensions and the vortex coordinate system with its origin at the trailing edge tip are shown in Fig. 6 while more details of the model are given in Ref. 5.

Effect of Variation of Angle of Attack

For the CV-990 model, $u_{\theta\ max}/V_\infty$, a/b and $u_{x\ min}/V_\infty$ are functions of α as shown in Fig. 7. Comparison of Fig. 7 with Fig. 3 for the rectangular wing shows a number of striking differences. For the CV-990 model, $u_{\theta\ max}/V_\infty$ only increases up to $\alpha = 8°$ and thereafter decreases whereas for the rectangular wing the values of $u_{\theta\ max}/V_\infty$ increased steadily up to $\alpha = 12°$. The core size, a/b, increases with α for the CV-990 model whereas it was independent of α in the rectangular model. All axial velocities measured for the CV-990 model were less than V_∞ and, as seen in Fig. 7, the minimum velocity decreases until it reaches a value of 90% of mainstream velocity.

The direct comparison between Figs. 3 and 7 is not straightforward since the model has been changed from a rectangular planform to an aircraft with fuselage, engine nacelles and antishock bodies, as well as having a wing with sweep, taper, and twist. The rectangular planform wing was relatively free of flow separation up to $\alpha = 12°$, whereas the CV-990 model exhibited separated flow above about $\alpha = 4°$ as evidenced by a reduction in lift curve slope and a sharp increase in drag with lift. The simplest explanation of Figs. 3 and 7 is that the additional drag of the CV-990 model results in a progressive increase in core size, a reduction in tangential velocity magnitudes, and a decrease in axial velocity, and that these effects become more pronounced as α is increased.

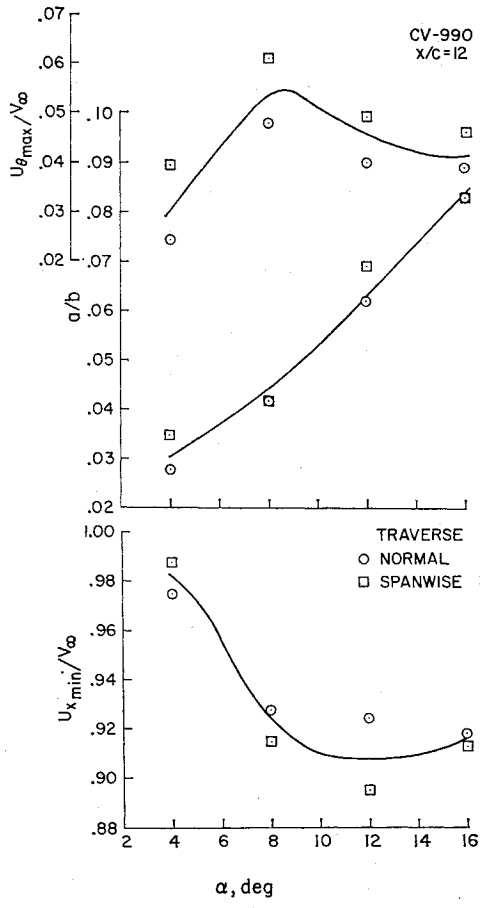

Fig. 7 CV-990, effect of variation of α, on $u_{\theta\ \max}$, a, and $u_{x\ \min}$, at $x/c = 12$.

Downstream Variation

One of the main concerns in wake turbulence is the persistence or downstream variation of the vortex flowfield. The variation of $u_{\theta\ \max}/V_\infty$, a/b, and $u_{x\ \min}/V_\infty$ are shown as functions of x/c in Fig. 8. We see that for the CV-990 model, $u_{\theta\ \max}/V_\infty$ decreases while a/b and $u_{x\ \min}/V_\infty$ increase with x/c. Again comparing the two models (Figs. 8 and 4)

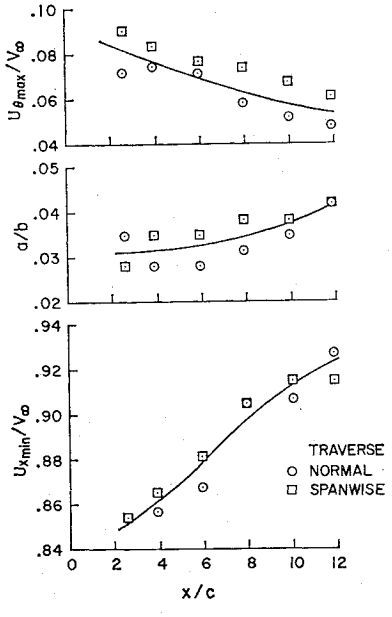

Fig. 8 CV-990, effect of variation of axial distance on $u_{\theta\ \max}$, a, and $u_{x\ \min}$ at $\alpha = 8°$.

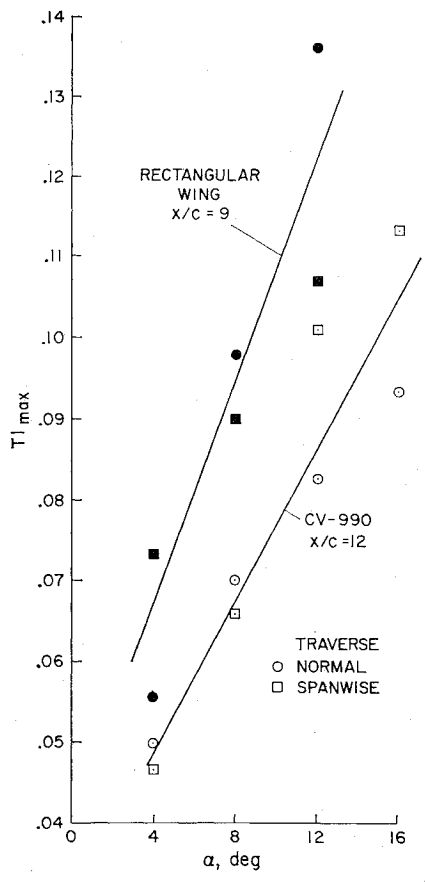

Fig. 9 Effect of variation of α on maximum value of turbulence intensity CV-990 $x/c = 12$, rectangular wing $x/c = 9$.

it is seen that beyond $x/c = 4$ both models show decay of $u_{\theta\ \max}/V_\infty$ with corresponding increases in core size a/b. The major differences are seen in the axial velocities that are above V_∞ for the rectangular wing, below V_∞ for the CV-990 model, and, in both cases, tending towards V_∞ as x/c is increased.

Turbulence Intensity

Classical models of trailing vortices do not take into account the possible presence of turbulence in the vortices. As the persistence of vortices many miles behind aircraft began to be reported, coupled with photographs of vortex contrails and smoke visualization of vortices behind aircraft in flight, it appeared that the rate of mixing of material within the vortex with the surrounding atmosphere was very small. The measurements of turbulence intensity obtained from the rms voltmeter readings of the three-wire anemometer show that the turbluence intensity is low, less than 1%, outside the core region, and that this increases to reach a maximum value at, or close to, the vortex center. These maximal values are plotted as functions of α for both models in Fig. 9. Turbulence intensity increases directly with α and reaches values of 11% for the CV-990 model at $\alpha = 16°$ and 12% for the rectangular model at $\alpha = 12°$.

These relatively high values of turbulence intensity would normally be associated with high rates of turbulent momentum and mass exchange that would act against the persistence of the vortices. It can only be concluded that the rotating flow confines the turbulence to a small central region and that it may even lead to damping of turbulence.[8]

Location of Vortex Centerline

The spanwise, y_c/b, and normal, z_c/b, locations of the vortex center, as determined from the point of zero tangential velocity

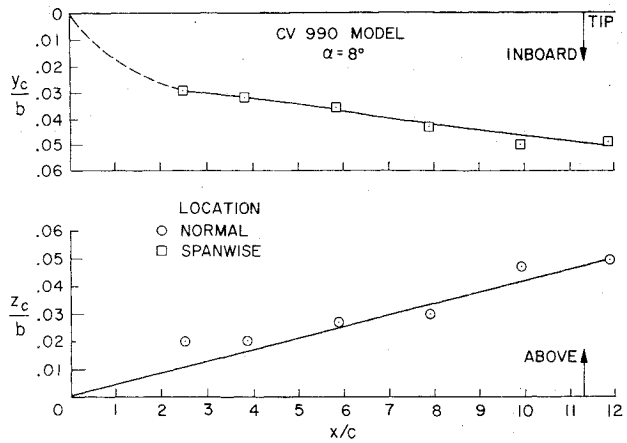

Fig. 10 CV-990, spanwise and normal location of vortex centerline as function of axial distance at $\alpha = 8°$.

are shown in Fig. 10 as functions of axial distance for the CV-990 model at $\alpha = 8°$. Comparing these values with those obtained for the rectangular wing (Fig. 5) it can be seen that the spanwise inboard movement of the vortex appears to be very similar for both models and that for both models the normal location is above the wing even for distances as far downstream as $x/c = 12$.

Effect of Flaps

Pilots have reported that, in their opinion, wake turbulence appeared to be less severe behind landing aircraft with trailing edge flaps deflected than behind aircraft with the trailing edge flaps undeflected. Figure 11 shows the effect of flaps on the velocity distributions at $x/c = 12$. The axial and tangential velocity components for a spanwise traverse were measured for the conditions of flaps undeflected and flaps deflected to 27° at 4° and 8° angle of attack. From the tangential velocity distribution the vortex can be seen to have been clearly displaced inboard and, for the angle of attack of 4°, the maximum tangential velocity increased as a result of the flap deflection. When the angle of attack was increased to 8° the core size increased and the maximum tangential velocity remained unchanged because of the flap deflection.

In the axial velocity distribution the effect of the flap deflection is to introduce a pronounced velocity defect at $\alpha = 4°$ whereas at the higher angle of attack, with the vortex more diffuse, the peak velocity defect was reduced and the region of reduced axial velocity increased. The data are insufficient to confirm or refute the pilot observations. At higher angles of attack, however, deflecting the flaps does tend to diffuse the vortex.

Comparison with Flight Tests

One of the main concerns in wake turbulence studies is to establish the far-flow vortex field. Flight measurements are difficult to make and this region is out of the range of wind tunnels. Some flight measurements made with a vortex meter in the wake of a Cherokee aircraft have been reported[9] as have velocity traverses made across the wake of a C5A (Ref. 10). These results are plotted in Fig. 12 and compared with the Ames wind-tunnel measurements. The values $u_{\theta\ max}/V_\infty$ have been divided by C_L since comparison is made for test conditions with varying lift coefficients and McCormick et al.[9] have shown $u_{\theta\ max}$ to be directly proportional to C_L. The values of x/b are plotted on a log scale to include measurements of both the near- and far-flowfields. From the results shown in Fig. 12 it may be concluded that the subsequent decay in tangential velocity beyond $x/b \approx 2$ is small. The wake can be thought of as made up of two regions, a roll-up

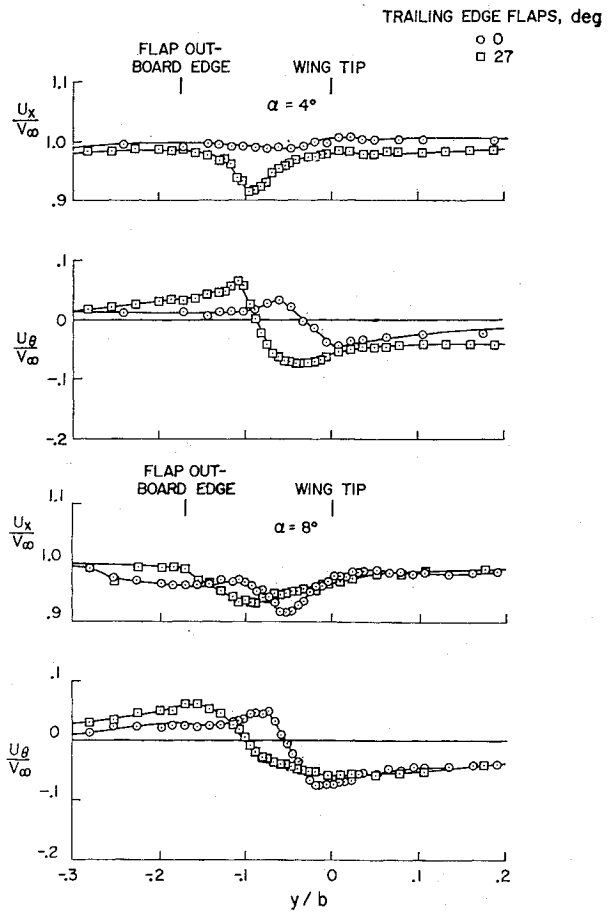

Fig. 11 CV-990, distributions of tangential and axial velocity for spanwise traverses. Comparison for trailing edge flap deflection 0° and 27°, $x/c = 12$.

region near the wing and a rolled-up region further downstream. The wind tunnel can be used to establish the initial condition for a computation of the turbulent vortex wake when the wind tunnel results are in the rolled-up region. An example of this computation is presented in Ref. 6.

There is a close association between the presence of axial velocities and the persistence of trailing vortices. Smoke visualization from towers during aircraft flybys show axial flows, generally towards the aircraft, but annular flows away from the aircraft have also been photographed.[1] Helium balloons, released from the ground[11] and subsequently entrained by the vortex by being centrifuged towards the

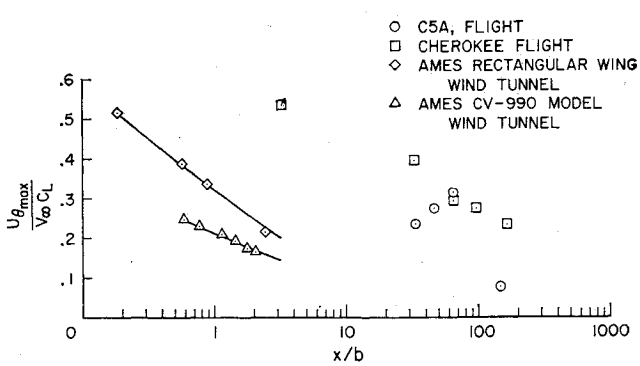

Fig. 12 Comparison between wind tunnel and flight test measurements of downstream variation of $u_{\theta\ max}$.

core, show axial flows of the order of 10% of flight speed. The few measurements of axial flows known to the authors have been assembled on Fig. 13. The Ames wind-tunnel data are those reported in this paper for the rectangular wing and CV-990 models; the wind-tunnel Cherokee wing model measurements were made with a pressure probe by Logan[12]; the helium balloon measurement in the wake of a Piper Apache aircraft were made by McCready[11] from movie film studies, and the flight test measurements in the wake of the C5A military transport and the C130 aircraft were made by pressure probe flight traverses across the aircraft wake as reported by Dunham.[10] The variety of conditions under which these measurements were made does not permit accurate conclusions to be drawn, but Fig. 13 summarizes the measurements of axial velocity to date.

Conclusions

The flowfields in the near wake region of a rectangular wing and a Convair 990 model aircraft have been measured in sufficient detail to establish the initial and boundary conditions of three-dimensional turbulent trailing vortex wakes. The measured velocity profiles show the relation between the classical potential and the real-fluid viscous vortex flow.

The over-all comparison of results obtained from the CV-990 aircraft model with those obtained with the clean rectangular wing shows that an increase in drag due to fuselage engine nacelles, anti-shock bodies, and flaps results in an increase in vortex core radius and magnitude of axial velocity defect, and a reduction in maximum tangential velocity.

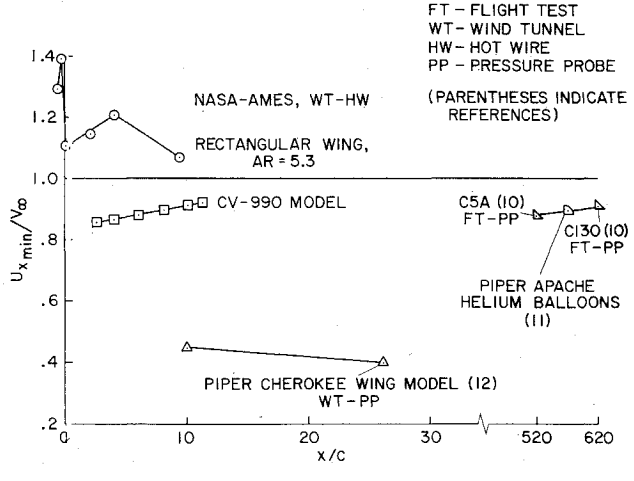

Fig. 13 Axial velocity measurements in near-flowfield (wind-tunnel tests) and far-flowfield (flight tests).

For the rectangular wing the maximum tangential velocity increases with angle of attack while core radius remains unchanged. For the CV-990 model the core radius increases with α but $u_{\theta\,max}$ decreases for values of α above 8°. Turbulence intensity up to approximately 12% was measured in the cores. Axial velocity defects in the core were measured at all angles of attack with the CV-990 model whereas with the rectangular wing axial velocity changed from a defect for $\alpha < 9°$ to an excess (thrust) for $> 9°$.

Deflection of flaps to 27° on the CV-990 model at $\alpha = 8°$ caused an increase in vortex core size and no change in maximum tangential velocities. Deflection of flaps also caused an inboard displacement of the vortex centerline. No answer is as yet available to the questions of the interaction of vortices with each other and the surrounding atmosphere and the relation between small scale wind-tunnel studies and full-scale flight tests.

References

[1] Olsen, J. H., Goldburg, A., and Rogers, M., eds., "Aircraft Wake Turbulence and its Detection," *Symposium on Aircraft Wake Turbulence*, Plenum Press, New York-London, 1971.

[2] Fage, A. and Simmons, L. F. G., "An Investigation of the Air Flow Pattern in the Wake of an Aerofoil of Finite Span," *Philosophical Transactions Royal Society (London)*, Ser. A, Vol. 225, No. 7, Jan. 1926.

[3] Corsiglia, V. R., Jacobsen, R. A., and Chigier, N. A., *An Experimental Investigation of Trailing Vortices Behind a Wing with a Vortex Dissipator, Aircraft Wake Turbulence and its Detection*, edited by J. H. Olsen et al., Plenum Press, New York-London, 1971, pp. 229–242.

[4] Chigier, N. A., and Corsiglia, V. R., "Tip Vortices—Velocity Distributions," TM X-62,087, Sept. 1971, NASA.

[5] Chigier, N. A. and Corsiglia, V. R., "Wind Tunnel Test Data for Wing Trailing Vortex Flow Survey—CV-990 Model and Rectangular Planform Wing," TM X 62-148, NASA.

[6] Kuhn, G. D., and Nielsen, J. N., "Analytical Studies of Aircraft Trailing Vortices, AIAA Paper 72-42, San Diego, Calif., 1972.

[7] Batchelor, G. K., "Axial Flow in Trailing Line Vortices," *Journal of Fluid Mechanics*, Vol. 20, No. 4, 1964, p. 645.

[8] Chigier, N. A., Beér, J. M., Grecov, D., and Bassindale, K., "Jet Flames in a Rotating Flow Field," *Combustion and Flame*, Vol. 14, 1970, pp. 171–179.

[9] McCormick, B. W., Tangler, J. L., and Sherrieb, H. E., "Structure of Trailing Vortices," *Journal of Aircraft*, Vol. 5, No. 3, May—June 1968, pp. 260–267.

[10] Dunham, E. R., Jr., Verstynen, H. A. Jr., and Benner, M. S., Unpublished Data, NASA Langley Research Center, Hampton, Va.

[11] MacCready, P. B., *An Assessment of Dominant Mechanisms in Vortex Wake Decay, Aircraft Wake Turbulence and its Detection*, edited by J. H. Olsen et al., Plenum Press, New York-London 1971, pp. 289–304.

[12] Logan, A. H., "Vortex Velocity Distributions at Large Downstream Distance," *Journal of Aircraft*, Vol. 8, No. 11, Nov. 1971, pp. 930–932.